

# Assessing the feasibility of increasing spatial resolution of remotely sensed image using HNN super-resolution mapping combined with a forward model

Nguyen Quang Minh\*

*Faculty of Surveying and Mapping, Hanoi University of Mining and Geology*

Received 03 September 2012

Revised 24 September 2012; accepted 15 October 2012

**Abstract.** Spatial resolution of land covers from remotely sensed images can be increased using super-resolution mapping techniques for soft-classified land cover proportions. A further development of super-resolution mapping techniques is downscaling the original remotely sensed image using super-resolution mapping techniques with a forward model. In this paper, the model for increasing spatial resolution of remote sensing multispectral image is tested with real SPOT 5 imagery for an area in Bac Giang Province, Vietnam in order to evaluate the feasibility of application of this model to the real imagery. The soft-classified land cover proportions obtained using a fuzzy *c*-means classification are then used as input data for a Hopfield neural network (HNN) to predict the multispectral images at sub-pixel spatial resolution. Visually, the resulted image is compared with a SPOT 5 panchromatic image acquired at the same time with the multispectral data. The predicted image is apparently sharper than the original coarse spatial resolution image.

**Keywords:** Hopfield neural network optimisation, soft classification, image downscaling, forward model.

## 1. Introduction

Spatial resolution of image and photos can be increased by the super-resolution algorithms. In the image processing context, image super-resolution commonly refers to the process of using a set of cross-correlated coarse spatial resolution images of the same scene to obtain a single higher spatial resolution image. There are numerous studies on such super-resolution

mapping such as Elad and Feuer [1], Tipping and Bishop [2]. Although widely applied in image processing, these approaches are hardly applicable for super-resolution of remotely sensed multispectral (MS) imagery because of the lack of a sequence of images of the scene at the same or similar times. The only feasible application of the super-resolution approaches using image sequences is for hyperspectral imagery [3]. For other common multispectral remotely sensed imagery, only few methods for increasing the spatial resolution to sub-pixel

\* Tel: 84-982721243.

E-mail: [nguyenquangminh@humg.edu.vn](mailto:nguyenquangminh@humg.edu.vn)

level have been proposed such as a Point Spread Function-derived convolution filter [4], segmentation technique [5], and geostatistical method [6].

Sub-pixel spatial resolution land cover maps can be predicted using super-resolution mapping techniques. The input data for super-resolution mapping are commonly the land cover proportions estimated by soft-classification [7]. There is a list of super-resolution mapping techniques have been introduced including spatial dependence maximisation [8], linear optimisation techniques [9], Hopfield neural network (HNN) optimisation [10], two-point histogram optimisation [11], genetic algorithms [12] and feed-forward neural networks [13]. The supplementary data are also supplied to HNN to produce more accurate sub-pixel land cover maps such as multiple sub-pixel shifted image [14], fused and panchromatic (PAN) imagery [15,16]. These latter approaches produce a synthetic MS or PAN image as an intermediate step for super-resolution mapping based on a forward model and then these images are compared with the predicted and observed MS or PAN images to produce an accurate sub-pixel image classification.

The creation of the predicted MS and then PAN image by a forward model suggested a possibility to implement a super-resolution for the MS image. A method for increasing the

spatial resolution of the original MS image is introduced by Nguyen Quang Minh et al [17]. The new model is based on the HNN super-resolution mapping technique from unsupervised soft-classification combined with a forward model using local end-member spectra [15,16]. The method is examined with a degraded remote sensing image and both visual and statistical evaluations shown a good result. However, there still exist some concerns about the feasibility of the model because it is not tested in a more complicated landscape with different kinds of land cover features which are varying in sizes and shapes as well as spectral characteristics. This paper, therefore, is to implement the test of the algorithm in a complicated landscape.

## 2. General model

The proposed model is an extension of the super-resolution mapping approach based on HNN optimisation. The prediction of a MS image at the sub-pixel spatial resolution is based on a forward model with local spectra as was used in Nguyen et al., 2006 [15]. In addition to the goal functions and the proportion constraint of the HNN for super-resolution mapping, a reflectance constraint is used to retain the brightness values of the original MS image.

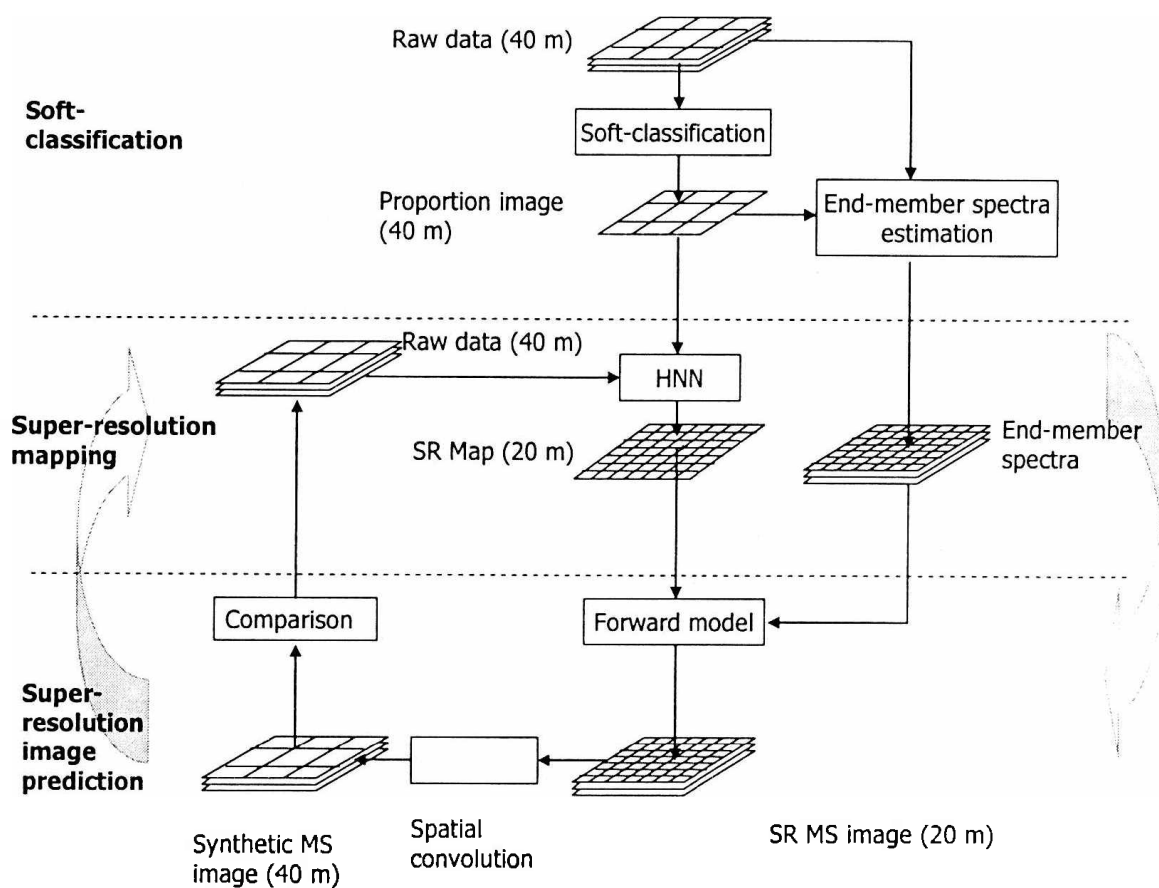


Figure 1. General model for super-resolution MS imagery prediction.

Figure 1 presents the HNN sub-pixel MS image prediction algorithm. The procedure is as follows: From the MS images at the original MS spatial resolution, land cover area proportion images are predicted using a soft-classifier. A set of local end-member spectra values is calculated based on the estimated land cover proportions and the original MS image. Land cover proportions are then used to constrain the HNN for super-resolution mapping with a zoom factor  $z$  to produce the land cover map at the sub-pixel spatial resolution. From the super-resolution land cover map at the first iteration, an estimated MS image (at the sub-pixel spatial resolution) is then produced using a forward model and the estimated local end-member spectra. The estimated MS image is then convolved spatially to create a synthetic MS image at the coarse

spatial resolution of the original image. Following a comparison of the observed and synthetic MS images, an error value is produced to retain the brightness value of the pixels of the original MS image. The process is repeated until the energy function of the HNN is minimised and the synthetic MS image is generated.

A demonstration of the algorithm for an image of  $2 \times 2$  pixels can be described in Figure 2. Firstly, the soft-classification predicts land cover proportion as in Figure 1b from the MS spectral image as in Figure 1a. There are two land covers in this image called Class A and Class B. From the land cover proportions in Figure 1b, the land cover classes at sub-pixel level are predicted as in Figure 1c where a pixel is divided into  $4 \times 4$  sub-pixels and the  $2 \times 2$  pixels image is super-resolved to  $16 \times 16$  pixels

land cover image of Class A and Class B. The brightness of the new  $16 \times 16$  pixels image is predicted using end-member spectra (standard brightness for the Class A and B in this area of the image). For example, the brightness of the pure pixel of Class A is 35 and Class B is 50

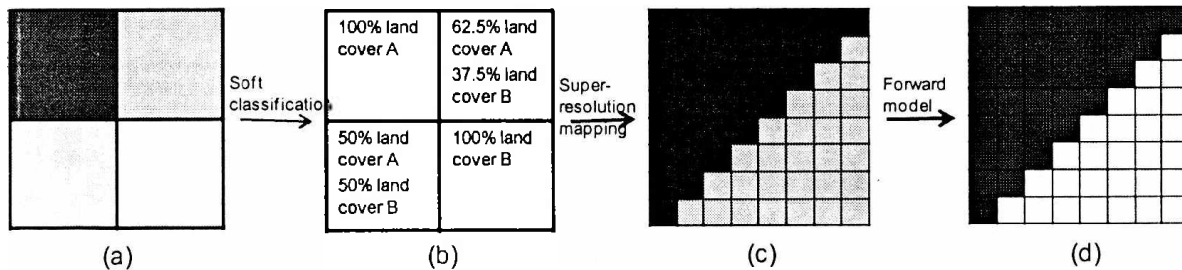


Figure 1. Creation of  $16 \times 16$  pixels image from  $2 \times 2$  pixels image.

### 2.1. Soft-classification for super-resolution mapping of MS imagery

Soft-classification is an intermediate step in the sub-pixel MS image prediction process. The prediction of the MS image based on super-resolution mapping requires land cover proportions which are obtained from soft-classification as input data. Conventionally, there must be a set of training data for most of the soft-classifiers. Accordingly, it is necessary to have some prior information about the spectral distribution of land cover classes in the MS bands, although training data are not always available for the image. And sometimes, there is a requirement of increasing the spatial resolution of the image without concerning the land cover classes in the image scene. In these cases, the algorithm can be implemented with unsupervised soft-classified land cover proportions such as fuzzy *c*-means classifier [18].

Supervised soft-classifiers could also be used, such as Bayesian, neural network or *k*-NN classifiers. However, the training data for these soft-classification techniques should be

and it is possible to produce a new spectral image by assigning all the sub-pixels belonging to Class A the brightness value of 35 and the sub-pixels of Class B the brightness value of 50 as in Figure 1d.

obtained from the unsupervised classifications. In the research implemented by Nguyen Quang Minh et al [17], a test for algorithm was implemented with a set of degraded MS image and soft-classified land cover proportions was obtained using *k*-NN classification using a training data set extracted from unsupervised Interactive Self-Organising Data (ISODATA) classifier. In this case, training data were clustered in the reference image. In this experiment, a fuzzy *c*-means classification is used to predict land cover proportions of a real SPOT image to produce super-resolved spectral image of different spatial resolutions to evaluate the algorithm.

### 2.2. Forward model and end-member spectra

After the first iteration of the HNN algorithm, once the sub-pixel classification is obtained, a forward model is used to produce a sub-pixel MS image from the sub-pixel land cover classes. The brightness value (e.g., reflectance, radiance, digital number) of a sub-pixel  $(m,n)$  of a spectral band  $s$  can be predicted as

$$R_{smn} = V_1 S_{s,1} + V_2 S_{s,2} + \dots + V_c S_{s,c} \quad (1)$$

where  $V_e$  is the output neuron of the class  $e$  and  $S_{s,e}$  is the end-member spectra of the land cover class  $e$  for a spectral band  $s$ . As presented in Nguyen et al., 2006 [15], the end-member spectra vector  $S_s$  ( $S_s = [S_{s,1}, \dots, S_{s,e}, \dots, S_{s,c}]$ ) of the original pixel  $(x,y)$  of the spectral band  $s$  can be estimated locally using the predicted land cover class proportions and the MS image at the original coarse spatial resolution as

$$S_s = (\mathbf{P}^T \mathbf{W} \mathbf{P})^{-1} \mathbf{W} \mathbf{P}^T \mathbf{R}_s, \quad (2)$$

where  $\mathbf{P}$  is a matrix of land cover proportions with

$$\mathbf{P} = \begin{bmatrix} P_1^{(x-1)(y-1)} & \dots & P_c^{(x-1)(y-1)} \\ \dots & \dots & \dots \\ P_1^{xy} & \dots & P_c^{xy} \\ \dots & \dots & \dots \\ P_1^{(x+1)(y+1)} & \dots & P_c^{(x+1)(y+1)} \end{bmatrix}$$

and  $\mathbf{W}$  is the matrix of weights with

$$\mathbf{W} = \begin{bmatrix} w^{(x-1)(y-1)} & 0 & 0 & 0 & 0 \\ 0 & \dots & 0 & 0 & 0 \\ 0 & 0 & w^{xy} & 0 & 0 \\ 0 & 0 & 0 & \dots & 0 \\ 0 & 0 & 0 & 0 & w^{(x+1)(y+1)} \end{bmatrix}$$



(a)



(b)

### 3. Experiment condition

#### 3.1. Data

The experiment in Nguyen Quang Minh et al [17] is conducted in an area having many large objects with linear boundaries. It may lead to a concern that the algorithm proposed in this paper is able to work well only with some specific landscapes. Therefore, a second data set is used for testing the algorithm in a more complicated landscape. This image was obtained in Bac Giang Province, Vietnam.

The SPOT 5 image used in this test was acquired in August 2011 with the spatial resolution of 10m and four spectral bands (Figure 2). The test image is registered to WGS-1984 UTM map projection in Zone 48N and the location is at 21°17'53.65"N, 106°11'7.64"E. The test image covers 1 square kilometre area of 102×102 pixels. To evaluate the results of increasing the spatial resolution algorithm, a 2.5m spatial resolution panchromatic image acquired at the same time was used (Figure 3b).

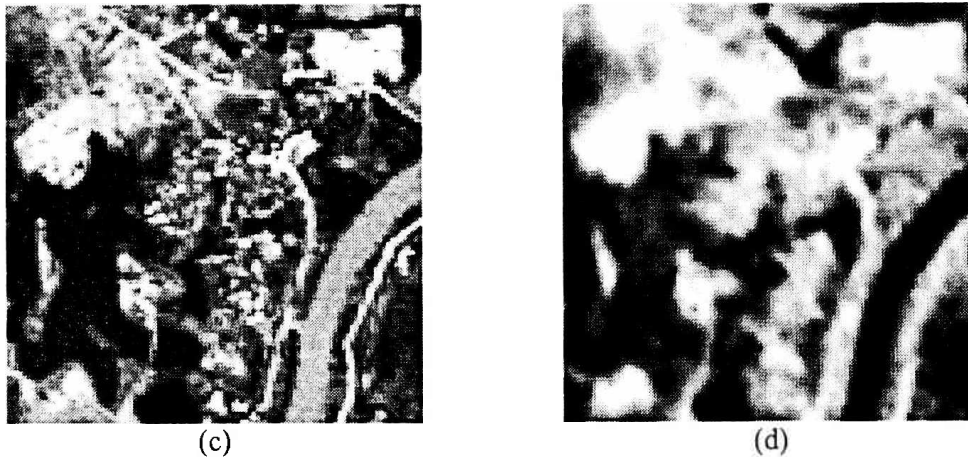


Figure 2. SPOT 5 image in Bac Giang Province, Vietnam: (a) Band 1, (b) Band 2, (c) Band 3 and (d) Band 4.

### 3.2. Soft-classification

The land cover proportions are estimated from 10m spatial resolution SPOT 5 image using fuzzy *c*-means classifiers so it is not necessary to have prior understanding about

land cover classes in the area. The soft-classified land cover proportions of five land cover classes and six land cover classes are obtained as in Figure 3c and Figure 3d, respectively.

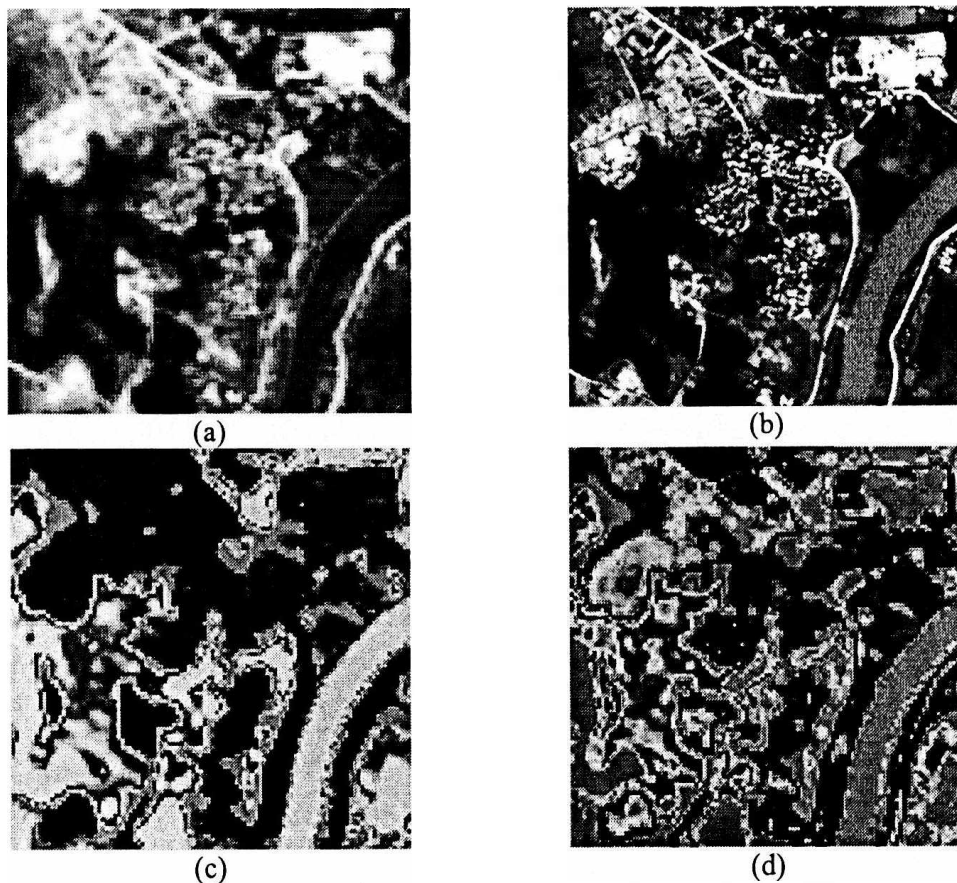


Figure 3. (a) original image, (b) Panchromatic image at 2.5m spatial resolution and land cover proportions from fuzzy *c*-means classification: (c) 5 land cover classes and (d) 6 land cover classes.

## 4. Results and discussions

### 4.1. Results

The method of increasing the MS image using HNN and forward model was applied to super-resolve the 10m SPOT 5 MS images to predict MS image at spatial resolutions of 5m (zoom factor of 2), 3.3m (zoom factor of 3) and

2.5m (zoom factor of 4). The predicted soft-classified proportions were used to constrain the HNN with weighting factors of  $k_1 = 100$ ,  $k_2 = 100$ ,  $k_3 = 100$  and  $k_4 = 100$  to predict the sub-pixel land cover and then the MS image. The false colours compositions using Band 1, Band 2 and Band 4 as Red, Green and Blue are shown in Figure 4.

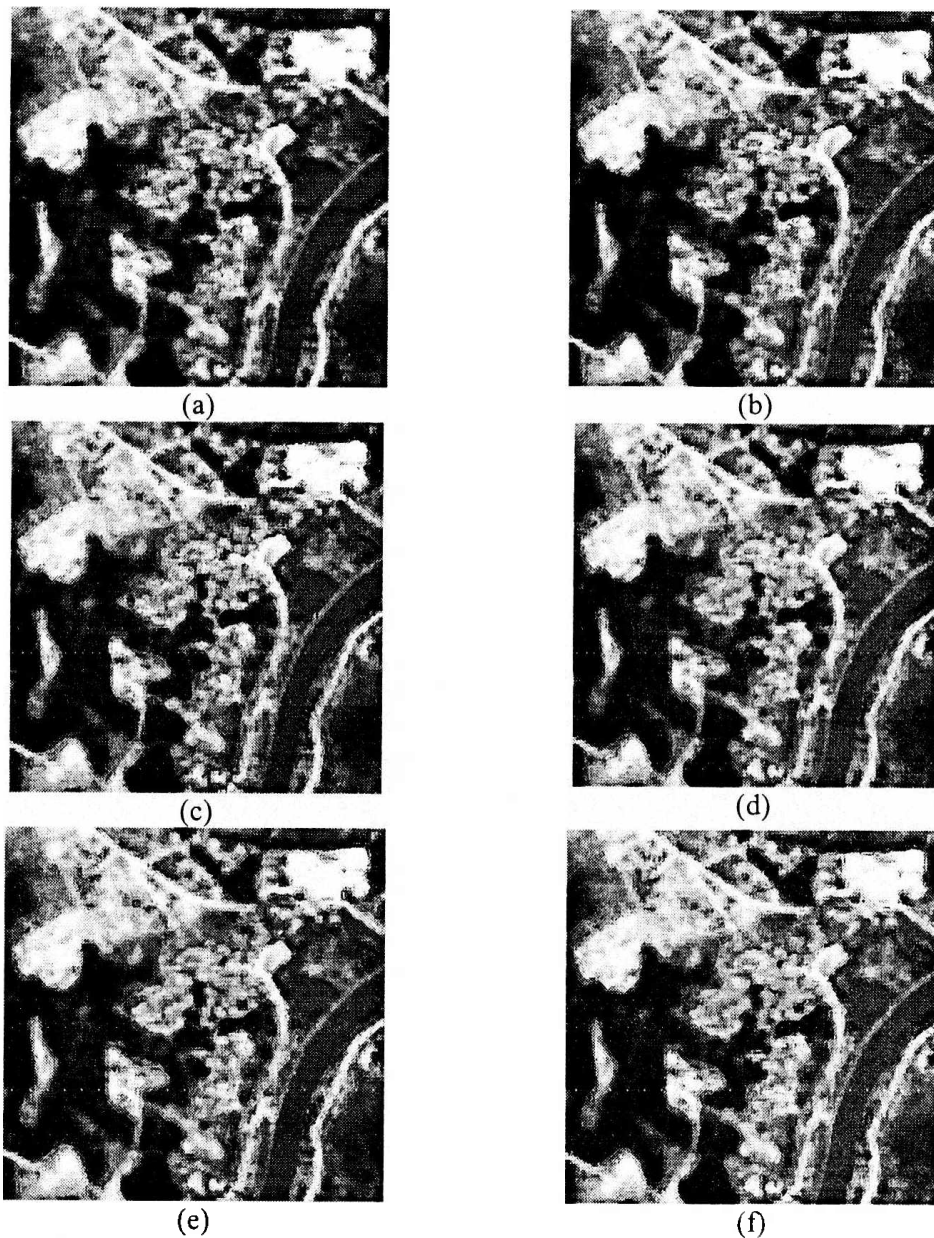


Figure 4. Super-resolution of 10m SPOT 5 multispectral image: (a) 5m super-resolved image using 5 land cover classes, (b) 3.3m super-resolution image using 5 land cover classes, (c) 2.5m super-resolution image using 5 land cover classes, (d) 5m super-resolution image using 6 land cover classes, (e) 3.3m super-resolution image using 6 land cover classes, and (f) 2.5m super-resolution image of 6 land cover classes.

#### 4.2. Evaluation

In the case of degraded image as in Nguyen Quang Minh et al. [17], the downsampled imagery was compared with the reference multispectral image at finer spatial resolution to obtain visual and qualitative evaluations. In this experiment, the finer multispectral imagery is not available for the full assessment. Therefore, the predicted multispectral image at finer resolution can be only compared with 2.5m panchromatic image for a visual evaluation.

The visual comparison of the super-resolved image from the real SPOT 5 data with the panchromatic image (Figure 3b) also shows an improvement in sharpness of the results. The objects in Figure 4(a-f) are sharpened and look

clearer than that of original image (Figure 3a). Although the landscape of image area is complicated with small and linear features such as houses and roads, the improvement of the algorithm can be seen in the boundaries of between the objects. Figure 5 shows the improvement of the algorithm for increasing the spatial resolution of MS image using HNN with a forward model to the original image. The boundaries of ponds in the centre of the original MS image (Figure 5a) are blurred and fragmented because of the mixing of the land categories in these boundary pixels. In the predicted MS image using HNN and a forward model (Figure 5b), these boundaries are clear and look more similar to the real ponds in panchromatic image (Figure 5c).

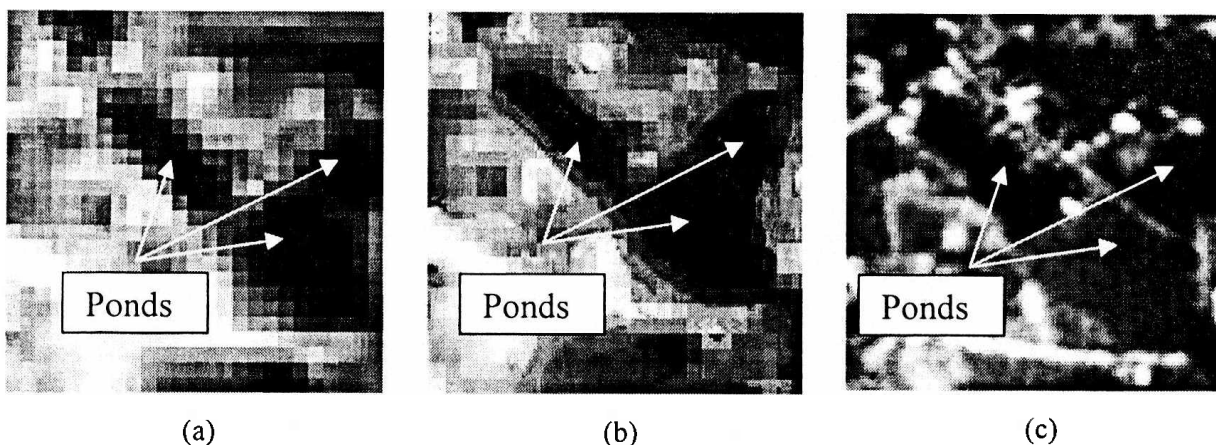


Figure 5. Some land cover features in (a) original MS image (false colour composite), (b) increased resolution MS image to 2.5m spatial resolution from 5 land cover class proportions (false colour composite) and (c) panchromatic image.

For small objects such as houses and roads, there are few objects which is not clearly seen in the original image can be recognised in the super-resolved image. In Figure 6a (composite image using Band 1, Band 2 and Band 4 of the original MS image), the road is difficult to be recognised because it is fragmented due to the mixed pixels effect. Using the HNN super resolution mapping and then the forward model

as in Figure 6b (composite image using Band 1, Band 2 and Band 4 of the 2.5m spatial resolution increased image), it is possible to recreate the road similar to the shape of the real road shown in the panchromatic image Figure 6c.

For the small features such as a group of houses in Figure 6c, the performance of the algorithm is not as good as that for the road.

However, the newly proposed algorithm still shows some improvement in defining clear boundaries of these features. This may be because of the soft-classifier cannot define the houses as a separate class. This problem may be

resolved by increasing the number of classes for fuzzy *c*-means classifier or using prior information on these classes in supervised soft-classifiers.

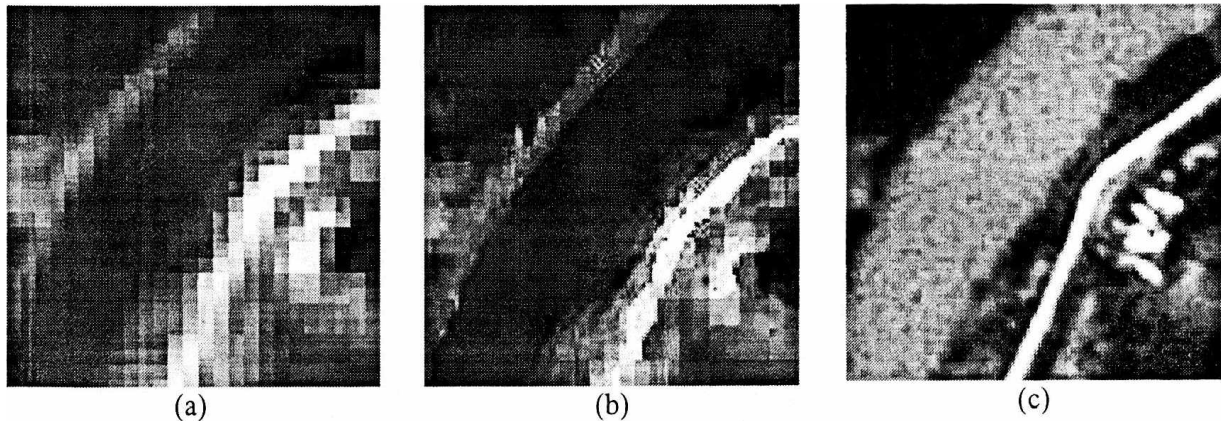


Figure 6. Some land cover features such as roads and houses in (a) original image, (b) spatial resolution increased image (false colour composite) and (c) panchromatic image.

#### 4.3. Discussions

The effect of zoom factor to spatial resolution increasing algorithm can be seen in Figure 8. . Comparing the image created by HNN using zoom factor of 2 (Figure 4a), with the image created with zoom factor of 3 (Figure 4b) and 4 (Figure 4c), it is possible to see that

when the zoom factor increases, the boundaries between the features are smoother. The boundaries between the ponds and the surrounding features are fragmented in Figure 8. a and Figure 8. b and look smoother and clearer in Figure 8. c.

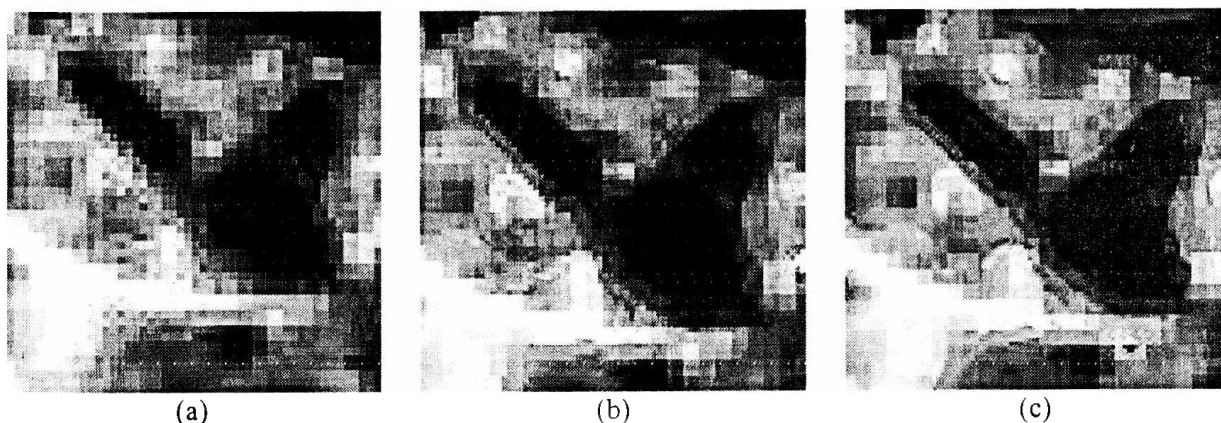


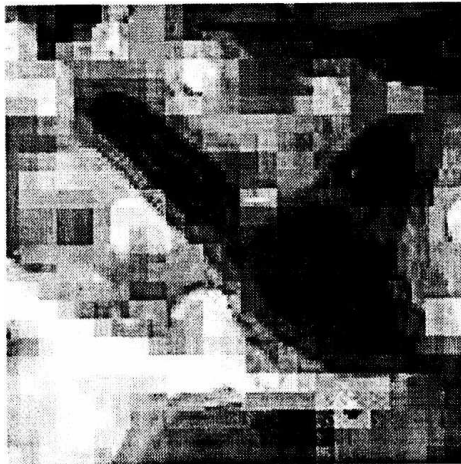
Figure 8. Effect of zoom factor to spatial resolution increasing algorithm: (a) zoom factor of 2, (b) zoom factor of 3 and (c) zoom factor of 4.

In spite of increasing the spatial resolution of the remotely sensed MS images, the proposed method has a problem with pixels that

belong to the same class (referred to as pure pixels in this paper). Although the problem can be partly solved by increasing the number of

classes so there more mixed pixels or dividing a class into sub-classes so several pure pixels are defined as mixed pixels, there will still exist pure pixels. The effect of number of land cover classes can be seen in Figure 9.. The ponds in Figure 9.a apparently smaller than those in

Figure 9.b due to some “pure pixels” in the boundaries were re-classified as mixed pixels when the number of classes increased from 5 to 6. These mixed pixels are then super-resolved to produce different boundaries between the same features in the two images.



(a)



(b)

Figure 9. (a) Result from HNN using 5 land cover classes, and (b) result from HNN using 6 land cover classes.

Because the HNN super-resolution method works only on mixed pixels, which are usually located across the border between different classes, it is suggested that the method is suitable for the super-resolution of images of large objects, for example the agricultural scenes. In these images, spatial variation is homogeneous within the land parcels and super-resolution based on the spatial clustering goal functions of the HNN can the agricultural field boundaries or increasing the sharpness of linear features such as roads or canals.

As mentioned above, the use of unsupervised classification can reduce the errors in land cover class proportion prediction. Furthermore, the use of unsupervised classification facilitates the automation of the spatial resolution increasing process because the class proportions can be obtained without training data and without a training step.

Through the choice of the number of classes, the user can control the effect of the super-resolution algorithm on the resulting sub-pixel MS images. When the number of classes is changed, the number of mixed pixels may be changed as a result.

A drawback of the HNN super-resolution procedure is the subjective choice of the parameters for the goal functions, the proportion constraint and the multi-class constraint [15]. By empirical investigation, the values of the parameters should retain an equal effect between the constraints and the goal functions in the optimisation process. For example, the empirical investigation in this paper shows that the values of these parameters in this paper were similar and around the value of 100. The finding is also obtained from the Nguyen Quang Minh et al [17].

## 5. Conclusions

The approach for increasing the spatial resolution MS imagery utilised the HNN super-resolution mapping technique combined with a forward model is tested with 10 SPOT 5 remotely sensed data. In this research, the soft-classified land cover proportions were estimated using a fuzzy *c*-means classifier. The feasibility of the method was evaluated based on visual comparison of the resulted image with panchromatic image acquired at the same time with original image. The comparison showed that the proposed method can generate MS images with more detail features. The super-resolved image was apparently sharper than the original coarse spatial resolution image. In addition, the evaluation also demonstrated that when the zoom factor increased, the resulting sub-pixel images were closer to the reference image.

## References

- [1] M. Elad and A. Feuer, Super-resolution reconstruction of image sequences, *IEEE Transactions on Pattern Analysis and Machine Intelligence*, vol. 21, pp. 817-834, 1999.
- [2] M. E. Tipping and C. M. Bishop, Bayesian image super-resolution in *Advances in Neural Information Processing Systems*, Boston, 2003.
- [3] T. Akgun, Altunbasak Y., and R.M. Mersereau, Super-resolution reconstruction of hyperspectral images, *IEEE Transactions on Image Processing*, vol. 14, pp. 1860-1875, 2005.
- [4] C. Pinilla Ruiz and J. Ariza Popez F., Restoring SPOT images using PSF-derived deconvolution filters, *International Journal of Remote Sensing*, vol. 23, pp. 2379-2391, 2002.
- [5] W. Schneider and J. Steinwendner, Land cover mapping by interrelated segmentation and classification of satellite images, *International Archives of Photogrammetry and Remote Sensing*, vol. 32, pp. part 7-4-3, 1999.
- [6] P. C. Kyriakidis and E. H. Yoo, Geostatistical prediction and simulation of point values from the areal data, *Geographical Analysis*, vol. 37, pp. 124-152, 2005.
- [7] G. M. Foody, Hard and soft classifications by a neural network with a nonexhaustively defined set of classes, *International Journal of Remote Sensing*, vol. 23, pp. 3853-3864, 2002.
- [8] P. M. Atkinson, Mapping sub-pixel boundaries from remotely sensed images, in *Innovation in GIS 4*, Z. Kemp (Ed.), Ed. London: Taylor & Francis, 1997, pp. 166-180.
- [9] J. Verhoeve and R. De Wulf, Land cover mapping at sub-pixel scales using linear optimisation techniques, *Remote Sensing of Environment*, pp. 96-104, 2002.
- [10] A. J. Tatem, H. G. Lewis, P. M. Atkinson, and M. S. Nixon, Super-resolution land cover pattern prediction using a Hopfield neural network, in *Uncertainty in Remote Sensing and GIS*, Foody G. M. and Atkinson P. M., Eds. London: John Wiley & Sons, 2002, pp. 59-76.
- [11] P.M. Atkinson, E. Pardo-Iguzquiza, and M. Chica-Olmo, Downscaling Cokriging for Super-Resolution Mapping of Continua in Remotely Sensed Images, *IEEE Transactions on Geoscience and Remote Sensing*, vol. 46 no. 2, pp. 573 - 580, 2008.
- [12] K. C. Merterms, L., Ducheyne, E. I. Verbeke, and R. De Wulf, Using genetic algorithms in sub-pixel mapping, *International Journal of Remote Sensing*, vol. 24, pp. 4241-4247, 2003.
- [13] K. C. Merterms, L. Verbeke, T. Westra, and R. De Wulf, Sub-pixel mapping and sub-pixel sharpening using neural network predicted wavelet coefficients, *Remote Sensing of Environment*, vol. 91, no. 2, pp. 225-236, 2004.
- [14] Feng Ling, Yun Du, Fei Xiao, Huaping Xue, and Sheng Jun Wu, Super-resolution land-cover mapping using multiple sub-pixel shifted remotely sensed images, *International Journal of Remote Sensing*, vol. 31, no. 19, pp. 5023-5040, 2010.
- [15] Q. M. Nguyen, P. M. Atkinson, and H. C. Lewis, Super-resolution mapping using Hopfield neural network with fused images, *IEEE Transactions on Geoscience and Remote Sensing*, vol. 44, no. 3, pp. 736-749, 2006.
- [16] Quang Minh Nguyen, Peter M. Atkinson, and Hugh G. Lewis, Super-resolution mapping using Hopfield Neural Network with panchromatic imagery, *International Journal of*

- Remote Sensing*, vol. 32, no. 21, pp. 6149-6176, 2011.
- [17] Quang Minh NGUYEN, Van Duong DO, P.M. Atkinson, and H.G.Lewis, Downscaling Multispectral Imagery Based on the HNN Using Forward Model, in *7<sup>th</sup> FIG Regional Conference on Spatial Data Serving People: Land Governance and the Environment-Building the Capacity*, Hanoi, 2009.
- [18] J. C. Bezdek, J. M. Keller, R. Krishnapuram, and N. R. Pal, *Fuzzy Models and Algorithms for Pattern Recognition and Image Processing*. Boston: Kluwer, 1999.
- [19] G. M. Foody, The role of soft classification techniques in the refinement of estimates of Ground Control Point location, *Photogrammetric Engineering and Remote Sensing*, vol. 68, pp. 897-903, 2002.